2026 IEEE International Conference on Robotics and Automation (ICRA 2026)
June 1-5, 2026. Vienna, Austria

Contributing Factors in Human-Robot Handshake: Compliance, Hand Grip, and Synchrony

Adnan Saood[1], Adriana Tapus[2]

Abstract— **Physical touch, such as handshakes, plays a critical role in human-robot interaction (HRI), influencing perceived naturalness and social presence. This study investigates how arm compliance, hand grip strength, and motion synchrony jointly affect the subjective quality of a human-robot handshake. We implemented a fully actuated, tactile-sensorized humanoid hand mounted on a manipulator arm and designed a compliant, oscillatory handshake controller with adaptive synchronization. Sixteen participants experienced handshakes across a 2x2x2 factorial design, varying arm compliance, grip strength, and synchrony. Objective kinematic analysis revealed significant main and interaction effects across all factors. At the same time, subjective ratings showed clear preferences for a weaker grip and greater arm compliance, with synchrony exerting minimal influence on perceived naturalness. These results highlight a perceptual hierarchy in HRI: foundational haptic properties exert the strongest influence on user experience, while advanced kinematic adjustments have limited impact when basic comfort is lacking. This insight provides concrete guidance for designing robotic handshakes that feel more human-like and pleasant.**

I. Introduction

Physical contact is a key element in social robotics, with tactile interactions like handshakes enhancing a robot's naturalness and perceived social presence [1]. The handshake, a culturally significant gesture involving prolonged contact, effectively conveys nuanced social cues [2]–[4], and initiating interactions with a handshake can foster cooperation and positive outcomes [5], [6]. In human–robot interaction (HRI), robotic handshakes can shape perceptions of warmth, likability, and social competence [7], [8], and insight into human hand morphology [9]. Furthermore, even quadruped robots have demonstrated the capacity to convey a sense of naturalness through handshakes or "paw" gestures [2], [10].

Implementing human-like handshakes presents technical challenges, primarily in achieving mechanical compliance and real-time sensory feedback. Compliance, the ability of the robot to yield and adapt to external forces, is critical for safety and user comfort, as overly stiff systems can exert excessive force or resist natural movements [3], [11], [12]. Unlike simple trajectory synchronization, compliance requires modulating the robot's impedance to mirror subtle human adjustments. Real-time adaptation also depends on accurately sensing the human partner's forces and motions, necessitating a sophisticated anthropomorphic end-effector with integrated force sensors and a soft structure [12]–[15], enabling secure yet comfortable interaction [16], [17].

The naturalness of a handshake further depends on human perception. Achieving human-like handshakes requires adaptive control responsive to the partner's timing, grip, and motion, with real-time compliance and synchronization being essential [3], [18], [19]. Social psychology demonstrates that synchronized behavior, through movement, posture, or subtle nonverbal mirroring, builds rapport, enhances positive emotions, and strengthens social bonds [20]–[24].

In HRI, synchronization extends beyond imitation: effective interaction requires the robot to align its actions intentionally and adaptively with human behavior [25], [26]. Timing mismatches can make handshakes feel awkward, whereas approaches using Central Pattern Generators (CPGs) to adapt motion and stiffness produce individualized, natural handshakes and even reveal social cues [18]. Tele-haptic studies further show that reproducing mutual grip forces rather than maintaining a rigid grip yields more realistic, synchronized interactions [27]. These findings underscore the need for handshake controllers integrating timing synchronization and adaptive compliance.

Robotic handshake research has explored embedding compliance through impedance/admittance control, distributed sensing, and adaptive stiffness. For example, [28] developed a gripper with proprioceptive sensing that estimates interaction forces in real time, enabling safe and adaptive handshakes. Grip modulation strongly influences perceived naturalness and comfort: tactile sensors that detect when to squeeze and release improve ratings [29], and compliant, gentle grips convey warmth and empathy [1]. Synchronization and bidirectional haptic coordination also enhance realism [27], [29].

Despite these advances, most studies address compliance, grip modulation, or synchronization in isolation, leaving the combined effect on user perception largely unexplored. For example, [28] highlights compliant grasping for safety, [29] demonstrates improved naturalness through tactile squeeze timing, and [27] emphasizes mutual grip–force adaptation in tele-haptic handshakes. Recent work suggests that integrating compliance and grip control may yield richer interactions [30], with adaptive controllers learning preferred grip from human feedback. Our approach differs in two ways: we frame grip control in terms of compliance rather than force, and we employ a high-density silicone-based tactile array, improving interaction compared to the aluminum hand with 15 sensors used in [30].

*This work was supported by ENSTA, Institut Polytechnique de Paris, France

[1]Adnan Saood is a PhD fellow of U2IS, ENSTA, Institut Polytechnique de Paris, Paris, France adnan.saood@ensta.fr

[2]Adriana Tapus is a Full Professor in the Autonomous Systems and Robotics Lab/U2IS, ENSTA, Institut Polytechnique de Paris, Paris, France adriana.tapus@ensta.fr

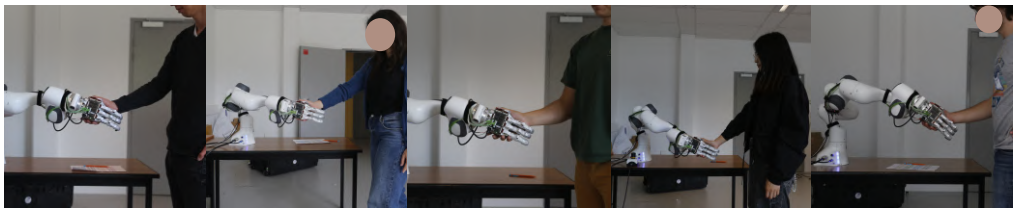

Fig. 1. Sixteen participants took part in the handshake experiment, which was conducted in a calm setting. Participants stood in front of the robot and performed handshakes upon instruction from the experimenter.

Fig. 2. Sensor array layout (left). Illustration of the sensor array covering the palm and fingers of the Meka M2 Robot hand (right).

These observations highlight the need for multi-factor experimental designs that systematically vary compliance, grip force, and synchronization to uncover interaction effects that single-factor studies cannot capture. Our study addresses this gap by using a factorial design that manipulates compliance, grip stiffness, and synchronization, providing insights for both HRI research and social robot design.

II. Methods

A. Robotic System Overview

The robotic system consists of the Meka M2 robotic hand with a tactile interface, mounted as an end-effector for the Franka Emika Panda (FEP) arm. The FEP is a lightweight, 7-axis collaborative robot arm designed for safe, direct interaction with people. Its integrated torque sensors on all joints provide a unique, human-like sensitivity.

B. Tactile 5 DoF Humanoid Hand End-Effector

The hand comprises five motors and four fingers. It is covered with a dense, in-house fabricated tactile sensor array consisting of 90 elements. The sensors operate at 512 Hz, and their real-time data is used to modulate the hand's grip during a handshake. The distribution of the tactile array elements on the hand is shown in Fig. 2.

C. Compliant and Synchronous Handshake

To control the arm motion, we used a classical joint-space impedance controller in which the desired joint torques, τ_d, are computed based on the impedance model, which is defined by the following decoupled relationship for each joint:

$$\tau_d = \mathbf{K}(\mathbf{q}_d - \mathbf{q}) - \mathbf{D}\dot{\mathbf{q}} \tag{1}$$

Here, $\mathbf{q}$ and $\dot{\mathbf{q}}$ are the current joint position and velocity vectors, respectively, while $\mathbf{q}_d$ is the desired joint position vector. The diagonal matrices $\mathbf{K}$ and $\mathbf{D}$ denote the stiffness and damping gains, respectively. To ensure a smoother input for the damping term and to further enhance system stability, the measured joint velocity, $\dot{\mathbf{q}}$, is filtered using a first-order low-pass filter.

Handshake Trajectory Generation: The handshake motion was modeled as an oscillatory movement along a smooth path in the n-dimensional joint space:

$$\Gamma : s \in [0,1] \rightarrow \Gamma(s) \in \mathbb{R}^n \tag{2}$$

where s is a scalar path parameter. The desired joint trajectory $\mathbf{q}_d(t)$ is generated by moving along this path according to a parameter $s(t)$, which is driven by an oscillator with phase $\phi(t)$:

$$\mathbf{q}_d(t) = \Gamma\big(s(t)\big) \tag{3}$$

$$s(t) = s_c - E(t) s_a \cos\phi(t) \tag{4}$$

Here, $s_c \in [0,1]$ is the path's midpoint, $s_a \in [0,1]$ is the half-span of the traversal, and $E(t) \in [0,1]$ is the minimum-jerk envelope that smoothly ramps the motion amplitude at the beginning and at the end of the motion.

$$E(t) = \begin{cases} j(\tau), & \tau = \frac{t}{T_{1/2}},\ 0 \le t < T_{1/2} \\ 1, & T_{1/2} \le t \le T_{\text{tot}} - T_{1/2} \\ j(\hat{\tau}), & \hat{\tau} = \frac{T_{\text{tot}} - t}{T_{1/2}},\ T_{\text{tot}} - T_{1/2} < t \le T_{\text{tot}} \end{cases} \tag{5}$$

where $j(\tau) = 10\tau^3 - 15\tau^4 + 6\tau^5$.

This generates a smooth oscillatory trajectory that is passed to the joint trajectory impedance controller.

Synchronization Controller: Synchronization in our controller is defined as the minimization of apparent resistance. Algorithm 1 details the synchronization control procedure. In joint impedance control, apparent resistance is naturally measured as the difference between the commanded and actual joint positions, expressed as the error term in Equation 6.

$$\mathbf{e}_q(t) = \mathbf{q}(t) - \mathbf{q}_d(t) \tag{6}$$

The error is projected onto the path's tangent to obtain a phase-consistent error measure. The tangent is $\mathbf{g}(s) = \Gamma'(s)$, and the phase tangent (normalized derivative with respect to ϕ) is $(\partial \mathbf{q}_d / \partial \phi)(t) = \mathbf{g}(s(t))\, E(t)\, s_a \sin\phi(t)$, with normalized tangent direction in Equation 7.

$$b(t) = \frac{\frac{\partial \mathbf{q}_d}{\partial \phi}(t)}{\left\| \frac{\partial \mathbf{q}_d}{\partial \phi}(t) \right\| + \varepsilon} \tag{7}$$

where $\varepsilon > 0$ prevents division by zero. The tangential motion error of the robot is then expressed as shown in Equation 8.

$$e_t(t) = b(t)^\top \mathbf{e}_q(t) \tag{8}$$

This overall error is subsequently decomposed to address two distinct synchronization objectives. Temporal adaptation, which tunes the phase and frequency of the handshake, is handled through the phase-consistent error $e_t(t)$. Spatial adaptation, which refines the geometric shape of the path, is addressed using the generalized projection error $e_s(t)$ (see Equation 9).

$$e_s(t) = \frac{\mathbf{g}(s(t))^\top \mathbf{e}_q(t)}{\|\mathbf{g}(s(t))\|^2 + \varepsilon_s} \tag{9}$$

Remark: To enhance numerical stability, the phase-aligned error $e_t(t)$ and the generalized projection error $e_s(t)$ are low-pass filtered before being used in the adaptation laws. The filtered signals are denoted by $\tilde{e}_t$ and $\tilde{e}_s(t)$.

Temporal Synchrony Control Laws: The oscillator phase dynamics are adapted using $\tilde{e}_t(t)$:

$$\dot{\phi}(t) = \omega(t) + K_\phi \, E(t) \, \tilde{e}_t(t) \tag{10}$$

$$\dot{\omega}(t) = K_\omega \, E(t) \, \tilde{e}_t(t) - \lambda_\omega \big(\omega(t) - \omega_0\big) \tag{11}$$

with $K_\phi, K_\omega > 0$ (temporal synchrony gains) and $\lambda_\omega > 0$ (drift damping), and we impose hard bounds $\omega_{\min} \le \omega(t) \le \omega_{\max}$.

Spatial Synchrony Control Laws: We adapt the path midpoint s_c and path span s_a by gradient steps using $\tilde{e}_s(t)$:

$$\dot{s}_c = K_c \, E(t) \, \tilde{e}_s(t), \tag{12}$$

$$\dot{s}_a = -\, K_a \, E(t) \cos\phi(t) \, \tilde{e}_s(t). \tag{13}$$

with $K_c, K_a > 0$. We impose hard bounds

$$0 < s_{\min} \le s_c \le s_{\max} < 1 \tag{14}$$

$$0 < s_{a,\min} \le s_a \le s_{a,\max} \tag{15}$$

In both temporal and spatial synchrony control, we introduce a top-level term η, called the synchrony factor. All four adaptation constants $K_\phi, K_\omega, K_c, K_a$ are multiplied by η before controller activation so that the synchrony level is adaptable.

Special Case Demonstration: Straight line in joint space.: If $\Gamma_l(s) = (1-s)Q_1 + sQ_2$, where $Q_1, Q_2 \in \mathbb{R}^n$ are two points in joint space. One can set

$$C = \tfrac{1}{2}(Q_1 + Q_2) \tag{16}$$

$$A = \tfrac{1}{2}(Q_2 - Q_1) \tag{17}$$

$$q_d(t) = C - E(t) \, A \cos\phi(t) \tag{18}$$

Here, C represents the midpoint (bias) of the handshake trajectory, while A represents the oscillation amplitude.

Algorithm 1 Compliant and Synchronous Handshake Control

Initialize $\phi(0)$, $\omega(0) = \omega_0$, s_c, s_a
for $0 \le t \le T_{tot}$ **do**
  Measure joint state $(\mathbf{q}(t), \dot{\mathbf{q}}(t))$
  Filter velocity:

$$\dot{\mathbf{q}}_f[k] = (1-\alpha)\dot{\mathbf{q}}_f[k-1] + \alpha \dot{\mathbf{q}}[k]$$

  Compute envelope $E(t)$
  Generate desired trajectory:

$$\mathbf{q}_d(t) = \Gamma(s(t)), \quad s(t) = s_c - E(t) s_a \cos\phi(t)$$

  Compute error: $\mathbf{e}_q(t) = \mathbf{q}(t) - \mathbf{q}_d(t)$
  Project errors:

$$e_t(t) = b(t)^\top \mathbf{e}_q(t), \qquad e_s(t) = \frac{\mathbf{g}(s(t))^\top \mathbf{e}_q(t)}{\|\mathbf{g}(s(t))\|^2 + \varepsilon_s}$$

  Low-pass filter $e_t, e_s \mapsto \tilde{e}_t, \tilde{e}_s$
  Update phase dynamics:

$$\dot{\phi} = \omega + K_p E(t) \tilde{e}_t, \qquad \dot{\omega} = K_\omega E(t) \tilde{e}_t - \lambda_\omega(\omega - \omega_0)$$

  Update path parameters:

$$\dot{s}_c = K_c E(t) \tilde{e}_s, \qquad \dot{s}_a = -K_a E(t) \cos\phi(t) \tilde{e}_s$$

  Apply impedance torques
end for

The bias and amplitude adaptations then simplify to the standard joint-space laws:

$$\dot{C} = K_c E(t) \, \tilde{e}_s(t) \tag{19}$$

$$\dot{A} = -K_a E(t) \cos\phi(t) \, \tilde{e}_s(t) \tag{20}$$

A one-degree-of-freedom (DoF) simulation of the synchrony controller is illustrated in 3.

It is possible to adapt the geometric shape of the joint-space trajectory Γ. We parametrize Γ by a finite parameter vector θ (e.g., control points, affine pose, or low-rank basis) and update θ by gradient descent on the instantaneous squared tracking error. The resulting law $\dot{\theta} = K_\theta J_\Gamma(s,\theta)^\top e_q$ (J is the Jacobian with respect to the parameters) generalizes both the earlier tangential-only adaptations (when $\theta = (s_c, s_a)$) and the straight-line full joint space adaptation when $\theta = (C, A)$. Regularization, damping, and projection ensure that the adaptations remain physically safe and bounded.

III. Experimental Design

The goal of this study is to explore how different compliance levels in a robot's arm and grip (i.e., hand compliance and grip strength), and handshake synchrony affect the perceived naturalness of a human-robot handshake. Specifically, we aim to investigate how these kinematic parameters influence:

- Motion synchronization.
- Force distribution and tactile comfort.
- Subjective human perception (i.e., naturalness, comfort, and human-likeness)

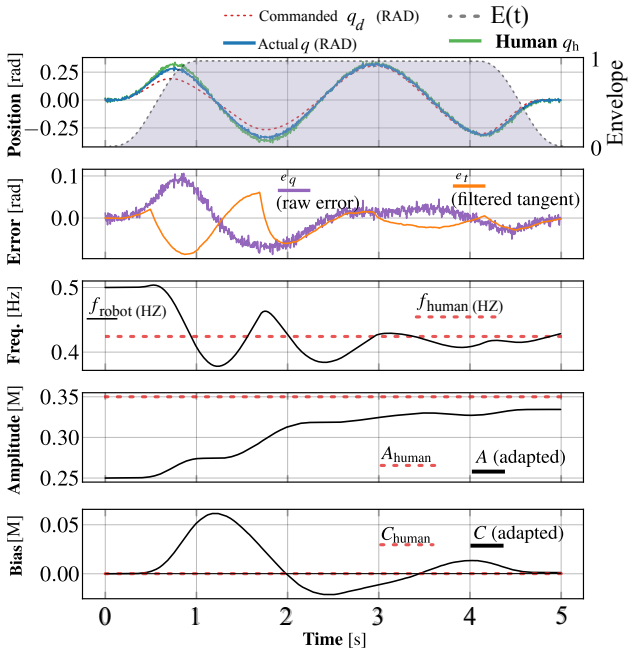

Fig. 3. **1-DoF simulation of a handshaking synchronous controller.** The top plot shows the commanded joint position (red dashed) converging toward the actual joint position (blue) to track the human input (green). The grey dashed line represents the envelope $E(t)$. The second plot shows the tracking error, both raw (e_q, purple) and filtered tangent ($\bar{e}_t$, orange), which reflects the apparent interaction force. The third, fourth, and fifth plots illustrate the adaptation of the handshake descriptors: frequency, amplitude, and bias, respectively. The robot gradually adjusts these parameters to synchronize with the human, reducing interaction forces and achieving coordinated motion by the end of the brief handshake.

A. Participants

A total of 16 participants (10 men, 6 women; mean age 27.0 $\pm$ 8.9 years, range 20–54) took part in the study. Participants originated from Europe (n = 10), Africa (n = 4), and Asia (n = 2). Personality was assessed with a short 10-item Big Five inventory [31] administered on a 5-point Likert scale; items were mapped to the five traits (i.e., openness, conscientiousness, extraversion, agreeableness, neuroticism).

B. Experimental Design and Conditions

To investigate these effects, we employ a $2\times2\times2$ factorial design with three independent variables: **Arm Compliance** (Low, High), **Hand Grip Strength** (Weak, Strong), and **Synchrony** (Not Present, Present).

This creates eight experimental conditions, as detailed in Table I.

TABLE I

EXPERIMENTAL CONDITIONS FOR THE $2 \times 2 \times 2$ FACTORIAL DESIGN.

Condition	Arm Compliance	Hand Grip Strength	Synchrony
C1	High	Weak	Not Present
C2	High	Strong	Not Present
C3	Low	Weak	Not Present
C4	Low	Strong	Not Present
C5	High	Weak	Present
C6	High	Strong	Present
C7	Low	Weak	Present
C8	Low	Strong	Present

1) Operationalization of Independent Variables:

- **Arm Compliance**: We tune the compliance of the robot arm by selecting impedance stiffness matrix K as follows $K_{\text{low}} = \text{diag}(150, 150, 150, 150, 10, 6, 2)$, $K_{\text{high}} = \text{diag}(20, 20, 20, 20, 10, 6, 2)$
- **Hand Grip Strength**: Weak and Strong grips are defined as 30% and 75% of the highest possible force the Meka M2 robot hand can apply. Grip Force is controlled using the tactile array.
- **Synchronization**: We define the conditions with label "No Synchrony" to have the synchronization controller gains set to zero, with the robot not adapting its handshake trajectory with the user at all. We define the label "Synchrony" with the robot adapting its commanded joint trajectory to the user's handshake trajectory using the synchrony controller.

C. Procedure

Participants first received an informed consent form in a quiet laboratory setting. After providing consent, they completed preliminary questionnaires to collect demographic information (height, gender, ethnicity), assess personality traits using the short Big Five Inventory [31], and record their current mood with the Pick-A-Mood test [32]. Figure 1 shows a subset of participants interacting with the experimental setup, which includes a robot arm and the Meka M2 robot hand.

The experiment consisted of a series of handshake interactions with a robotic arm. The session comprised eight distinct experimental conditions (see Table I), representing a full factorial design of the three independent variables. The presentation order of the conditions was randomized for each participant to mitigate potential order effects. During each trial, the robot initiated an up-down oscillatory handshake movement. Each interaction was designed to last approximately 5 to 8 seconds, a duration chosen to more closely reflect the brevity of natural human handshakes compared to the extended interactions used in some prior HRI studies. Immediately following each handshake, participants were prompted to provide subjective feedback on five questions assessing Naturalness, Comfort, Human-Likeness, Fluidity, and Pleasantness:

- Please evaluate the following statements:
  - The handshake was natural
  - The interaction was physically comfortable
  - The handshake was human-like
  - The handshake was fluid
  - The handshake was pleasant

After completing all eight conditions, participants took part in a semi-structured interview to collect qualitative insights, focusing on factors that contributed to a natural or unnatural experience, their preferences, and any changes in perception over time.

D. Data Collection and Measures

To evaluate the quality of the handshake across conditions, we collected a combination of objective performance metrics,

subjective perceptual ratings, and user data.

1) Objective Metrics: The physical dynamics of the interaction were captured using the robot's onboard sensors. This provided a rich dataset for post-hoc analysis, including kinematic data such as the robot's joint positions and velocities, as well as kinetic data such as measured joint torques and estimated external forces at the end-effector. These objective measures allow for a quantitative characterization of interaction effort and motion smoothness.

2) Subjective Ratings: Subjective perceptions were measured after each individual handshake using a concise questionnaire. Participants rated their experience on five distinct 7-point Likert scales (1 = Strongly Disagree, 7 = Strongly Agree), assessing the handshake's perceived naturalness, comfort, human-likeness, fluidity, and overall pleasantness. The brevity of this instrument was a deliberate design choice to minimize participant fatigue, given its repeated administration throughout the experiment.

3) User Data: The demographic, personality, and mood data collected prior to the interaction serve as user variables. This supplementary information enables correlational analyses to examine how individual differences shape perceptions of the robotic handshake. Additionally, trial-by-trial subjective ratings are analyzed to identify patterns of user adaptation throughout the session.

IV. Results

A. Factorial Design Results for Kinematic Data

To kinematically assess the quality of human–robot handshakes, we introduce the Objective Comfort Index (OCI), an integrated measure combining control accuracy and motion smoothness into a single interpretable score. The root-mean-square torque error ($e_{\tau,\text{rms}}$) and root-mean-square jerk (j_{rms}) are incorporated with negative polarity, thereby prioritizing handshakes exhibiting lower tracking error and smoother transitions. Each constituent metric is z-score normalized across all conditions, polarity-adjusted, and subsequently aggregated to ensure that higher OCI values consistently indicate greater perceived comfort. By jointly capturing control fidelity and kinematic smoothness within this structured framework, the OCI provides a robust and physically interpretable benchmark for evaluating and comparing handshake conditions.

$$\text{OCI}^{u,c} = -\hat{e}^{\,u,c}_{\tau,\text{rms}} - \hat{j}^{u,c}_{\text{rms}} \tag{21}$$

where $\hat{e}^{u,c}_{\tau,\text{rms}}$ and $\hat{j}^{u,c}_{\text{rms}}$ are the z-score-normalized joint torque error and joint jerk for user u in condition c.

Before conducting the repeated-measures ANOVA, the normality assumption was assessed using the Shapiro–Wilk test on the residuals of each condition. Results indicated no significant deviations from normality ($0.087 \leq p \leq 0.65$ for all factors), confirming that the data met the assumption required for ANOVA. The repeated-measures ANOVA was conducted to examine the effects of Synchrony, Arm Stiffness, and Hand Stiffness (Grip) on the Objective Comfort Index (OCI). All three main factors had highly significant effects on comfort:

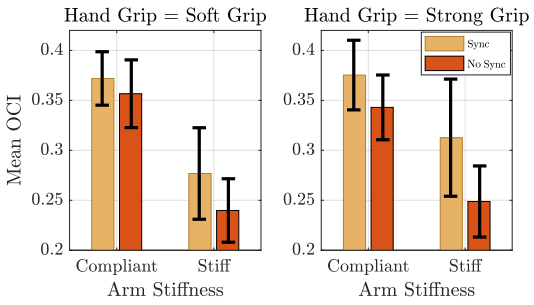

Fig. 4. Three-way interaction between Synchrony, Arm Stiffness, and Hand Stiffness on the Objective Comfort Index (OCI).

- Synchrony: $F(1,15) = 87.62, p < 0.001$
- Arm Stiffness: $F(1,15) = 56.19, p < 0.001$
- Hand Stiffness (Grip): $F(1,15) = 84.01, p < 0.001$

In addition to the main effects, all two-way interactions were significant:

- Synchrony×Arm Stiffness: $F(1,15) = 53.9, p < .001$
- Synchrony×Hand Stiffness: $F(1,15) = 83.7, p < .001$
- Arm Stiffness×Hand Stiffness: $F(1,15) = 43.1, p < .001$

Finally, the three-way interaction (Synchrony × Arm Stiffness × Hand Stiffness) was also significant, $F(1,15) = 48.88, p < 0.001$, indicating that the effect of one factor depends on the levels of the other two.

These results suggest that comfort is not determined by a single factor alone, but rather by the specific combination of synchrony and stiffness parameters. For instance, synchrony may significantly improve comfort when both arm and hand are compliant, but this effect may diminish when either or both are stiff.

Comfort is maximized under specific combinations of synchrony and stiffness. The interaction plots in Figure 4 illustrate these patterns, showing which combinations of arm and hand stiffness, with or without synchrony, produce the highest Objective Comfort Index (OCI). This highlights the importance of considering factor interactions when designing robotic or haptic systems for optimal user comfort.

B. User State

The distribution of the Big 5 personality traits among the participants is shown in Table II.

TABLE II
PERSONALITY TRAITS DISTRIBUTION OF THE PARTICIPANTS

Personality Trait	High	Low
Extraversion	7	9
Neuroticism	5	11
Agreeableness	13	3
Conscientiousness	11	5
Openness	10	6

Momentary affect, as assessed via the Pick-A-Mood task, exhibited substantial inter-individual variability (Tense/Nervous: n = 3; Excited/Lively: n = 2; Cheerful/Happy: n = 5; Calm/Serene: n = 5;

Bored/Weary: n = 1), indicative of a heterogeneous distribution of affective states at the time of assessment. Each mood rating was systematically located within the two-dimensional Activation–Pleasantness framework of the Pick-A-Mood test [32], thereby facilitating a fine-grained characterization of participants' affective profiles. Along the Activation dimension, participants were approximately evenly distributed between low (n = 6) and high (n = 10) activation levels. Along the Pleasantness dimension, the majority reported elevated pleasantness (n = 12), with a smaller subset indicating lower pleasantness (n = 4), suggesting an overall positively valenced affective context during the interaction period.

Across all factorial conditions (Grip Strength, Synchrony, Arm Compliance), analysis of correlations between personality traits, mood, and handshake quality scores (OCI, SRI) revealed no associations that met the predefined threshold for a strong correlation ($r > 0.55$) and statistical significance ($p < 0.05$). Similarly, no marginally significant correlations ($0.05 < p < 0.075$) exceeded this criterion. In contrast, strong and significant correlations ($r > 0.6$, $p < 0.05$) were observed between the self-reported quality dimensions themselves, specifically Naturalness, Comfort, Fluidity, and Pleasantness, highlighting internal consistency in participants' subjective ratings. Interestingly, Pleasantness did not correlate with Human-Likeness, suggesting that participants' enjoyment of the interaction was independent of how human-like the handshake felt.

While several traits (e.g., extraversion, neuroticism, conscientiousness) and mood states (activation) showed consistent moderate correlations with interaction ratings and cooperation indices ($r \approx 0.25$–0.44, all $p < 0.01$), these fell below the threshold for strong effects. Longer interactions with the robot and a larger sample size would likely enable the detection of these personality and mood influences more robustly.

C. Perceived Naturalness

To analyze the subjective ratings from the handshake interactions, we conducted a $2 \times 2 \times 2$ three-way repeated measures Analysis of Variance (ANOVA) on the average of reported items (Naturalness, Comfort, Human-Likeness, Fluidity, Pleasantness) for each user. We refer to it as the Subjective Rating Index (SRI).

The experimental factors were Arm Compliance (Low, High), Hand Grip (Weak, Strong), and Synchrony (Not Present, Present). The primary analysis was performed on the composite mean score across all five subjective questions.

The analysis revealed significant main effects for both Hand Grip and Arm Compliance in the Subjective Rating Index (SRI). However, no significant main effect was found for Synchrony, nor were any two-way or three-way interactions between the factors statistically significant. This indicates that the effects of grip and compliance on user perception were independent of each other and of the synchrony condition. The detailed findings are presented below.

D. Main Effect of Hand Grip

The strongest and most consistent factor influencing user perception was Hand Grip, which had a highly significant main effect on the Subjective Rating Index (SRI), $F(1, 15) = 15.25, p = 0.0014$. Post-hoc comparisons confirmed that the **Weak Grip** condition ($\mu = 4.65$, $\sigma = 1.20$) was rated significantly higher than the **Strong Grip** condition ($\mu = 3.39$, $\sigma = 1.57$). This preference for a weaker grip was statistically significant across all five individual subjective measures: Naturalness ($p = 0.0024$), Comfort ($p = 0.0024$), Human-Likeness ($p = 0.0021$), Fluidity ($p = 0.018$), and Pleasantness ($p = 0.021$). Users consistently preferred a weaker hand grip, which significantly enhanced perceptions of comfort, naturalness, human-likeness, fluidity, and pleasantness. This contrasts with the findings of [30], in which higher grip strength was preferred by participants. We suspect this difference is due to the larger and stronger form factor of the Meka M2 robot hand.

E. Main Effect of Arm Compliance

Arm Compliance also demonstrated a significant main effect on the average user rating ($F(1, 15) = 5.50$, $p = 0.033$). Participants reported a significantly better experience with the high compliance conditions ($\mu = 4.29$, $\sigma = 1.48$) compared to the low compliance conditions ($\mu = 3.75$, $\sigma = 1.39$). This finding was particularly evident in ratings of Naturalness ($p = 0.030$) and Pleasantness ($p = 0.025$), and was marginally significant for Comfort ($p = 0.055$). Thus, higher arm compliance led to a more positive user experience, particularly enhancing perceptions of naturalness and pleasantness.

Prior work has shown that increased mechanical compliance in robot arms or end-effectors often improves perceived comfort, safety, and user satisfaction [30], [33].

F. Absence of Synchrony and Interaction Effects

The main effect of Synchrony was not statistically significant ($F(1, 15) = 0.08$, $p = 0.781$), suggesting that the controller's synchronization with the user's motion did not measurably alter the subjectively reported quality of the handshake in this study. Furthermore, the analysis confirmed a complete absence of significant interactions. All two-way interactions (Compliance×Grip, $p = 0.940$; Compliance×Synchrony, $p = 0.893$; Grip×Synchrony, $p = 0.575$) and the three-way interaction (Compliance×Grip×Synchrony, $p = 0.930$) were non-significant. The lack of interactions is visually corroborated by the parallel trend lines in the interaction plots (see Figure 5). This simplifies the interpretation of the main effects, as the ideal setting for each parameter does not depend on the state of the others.

The detailed analysis of subjective ratings for each questionnaire item is illustrated in Figure 6, which presents the mean scores for Naturalness, Comfort, Human-Likeness, Fluidity, and Pleasantness across all eight experimental conditions. Consistent with the composite Subjective Rating Index results, users rated the Weak Grip significantly higher

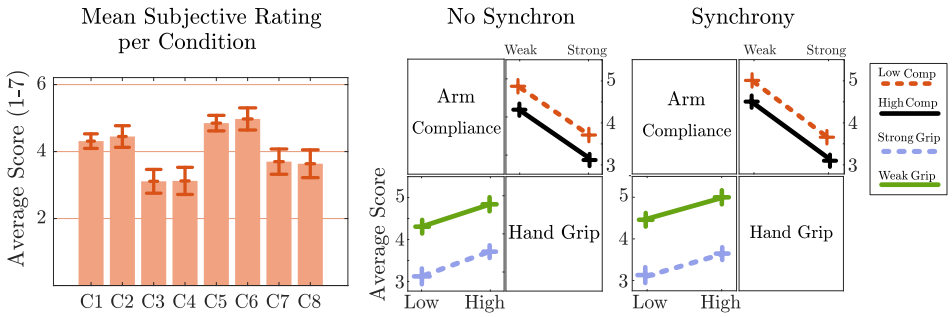

Fig. 5. Bar chart (Left) that represents the reported subjective comfort across the eight conditions. The results show a consistent preference for the Weak Grip over the Strong Grip and for High Compliance over Low Compliance across most subjective measures. Error bars represent the standard error of the mean. In interaction plots (Middle and Right), since no lines cross, they display the separation of interactions the users reported for three conditions.

than the Strong Grip for all five items, and High Compliance generally received higher scores than Low Compliance, particularly for Naturalness and Pleasantness. The star symbols under the question labels indicate statistical significance for the Grip and Compliance factors. These per-question ratings provide a nuanced view of how each factor individually influenced user perception, complementing the main effect trends shown in Figure 5.

V. Discussion and Conclusion

Our findings highlight a clear divergence between objective kinematic metrics and subjective user perceptions of a robotic handshake. Although synchrony, arm compliance, and grip jointly influence the objective comfort index (OCI), participants' preferences were straightforward: they consistently favored a gentle grip and a compliant arm, independent of synchronization.

We suggest a "haptic-first" perceptual model, in which users experience a handshake primarily through its core haptic cues. When these sensations are lacking, finer kinematic refinements such as synchrony provide little perceptual benefit. This hierarchy implies that designing human-robot interactions should first ensure basic haptic comfort before optimizing motion details. Kinematic data showed significant three-way interactions, indicating complex dependencies among parameters for optimal handshake dynamics. In contrast, subjective ratings revealed no interactions, suggesting that perceived naturalness is dominated by independent haptic factors. This decoupling simplifies design: focusing on grip and compliance optimization can yield stronger subjective evaluations than attempting to perfect complex kinematic interactions.

Personality traits and affect varied widely across participants, emphasizing that no single handshake configuration is optimal for everyone. However, given the high variability and the small participant pool, these findings cannot be generalized. Future work could investigate adaptive, personalized haptic tuning, where grip and compliance are adjusted according to individual traits or preferences. This study involved 16 participants and a single robot platform, limiting generalizability. Handshake duration and task context were also constrained. Future research could expand the participant pool, test different robotic hands, explore longer interactions, and integrate more nuanced social cues, such as gaze or posture, alongside haptic adaptation. Overall, our results underscore that tactile and force-based cues are the primary determinants of perceived naturalness in human-robot handshakes. Achieving a gentle, compliant touch is crucial, and only once this baseline is achieved do finer aspects such as motion and synchrony meaningfully enhance the interaction.

VI. Acknowledgment

We extend our gratitude to Andrea Rocchi, Hasson Cyril (X-Fab of École Polytechnique), and Thibault Toralba (U2IS of ENSTA) for their invaluable assistance and technical expertise. We are also deeply appreciative of the members and interns at U2IS and ENSTA for their support throughout the experimental phase of this research.

References

[1] M. E. Cansev, A. J. Miller, J. D. Brown, and P. Beckerle, "Implementing social and affective touch to enhance user experience in human-robot interaction," vol. 11, p. 1403679. [Online]. Available: https://www.ncbi.nlm.nih.gov/pmc/articles/PMC11345123/

[2] V. Prasad, R. Stock-Homburg, and J. Peters, "Human-robot handshaking: A review," vol. 14, no. 1, pp. 277–293. [Online]. Available: https://doi.org/10.1007/s12369-021-00763-z

[3] D. Mura, E. Knoop, M. G. Catalano, G. Grioli, M. Bächer, and A. Bicchi, "On the role of stiffness and synchronization in human–robot handshaking," vol. 39, no. 14, pp. 1796–1811, publisher: SAGE Publications Ltd STM. [Online]. Available: https://doi.org/10.1177/0278364920903792

[4] P.-H. Orefice, M. Ammi, M. Hafez, and A. Tapus, "Let's handshake and i'll know who you are: Gender and personality discrimination in human-human and human-robot handshaking interaction," in *2016 IEEE-RAS 16th Humanoids*, pp. 958–965.

[5] J. Schroeder, J. L. Risen, F. Gino, and M. I. Norton, "Handshaking promotes deal-making by signaling cooperative intent," *J. Pers. Soc. Psychol.*, vol. 116, no. 5, pp. 743–768, May 2019.

[6] C. Bevan and D. S. Fraser, "Shaking hands and cooperation in tele-present human-robot negotiation," in *2015 10th ACM/IEEE International Conference on Human-Robot Interaction (HRI)*, pp. 247–254, ISSN: 2167-2121. [Online]. Available: https://ieeexplore.ieee.org/document/8520651

[7] J. Avelino, F. Correia, J. Catarino, P. Ribeiro, P. Moreno, A. Bernardino, and A. Paiva, "The power of a hand-shake in human-robot interactions," in *2018 IEEE/RSJ International Conference on Intelligent Robots and Systems (IROS)*, pp. 1864–1869, ISSN: 2153-0866. [Online]. Available: https://ieeexplore.ieee.org/document/8593980

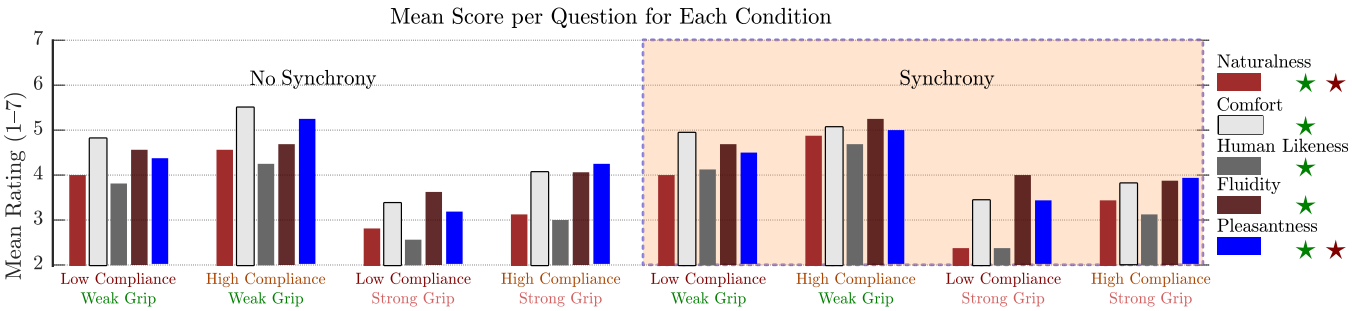

Fig. 6. Mean subjective ratings per question across all eight experimental conditions. Synchrony conditions are grouped with an orange background. No-Synchrony Conditions are grouped with a white background. Each bar represents the average score (1–7) given by 16 participants for one of the five questionnaire items ("Naturalness", "Comfort", "Human-Likeness", "Fluidity", "Pleasantness") in each condition, which are defined by the combination of Arm Compliance (Low/High), Hand Grip (Weak/Strong), and Synchrony (No Sync/Sync). The grouped bar chart allows comparison of question responses across conditions. Star symbols in the chart legend indicate statistical significance $p < 0.05$ for Grip (Green) and Compliance (Red) factors.

[8] P.-H. Orefice, M. Ammi, M. Hafez, and A. Tapus, "Pressure variation study in human-human and human-robot handshakes: Impact of the mood," in *2018 27th (RO-MAN)*, pp. 247–254, ISSN: 1944-9437.

[9] A. Saood and A. Tapus, "Human hand shape and grasping behavior estimation using a humanoid hand with a tactile interface," in *Social Robotics + AI*. Springer Nature Singapore, 2026, pp. 75–86.

[10] A. Chappuis, G. Bellegarda, and A. Ijspeert, "Learning human-robot handshaking preferences for quadruped robots." [Online]. Available: http://arxiv.org/abs/2406.19893

[11] A. Ghanbarzadeh and E. Najafi, "Safe physical human–robot interaction through variable impedance control based on ISO/TS 15066," vol. 19, no. 7, pp. 4741–4758. [Online]. Available: https://doi.org/10.1007/s12008-024-02074-9

[12] M. Arns, T. Laliberté, and C. Gosselin, "Design, control and experimental validation of a haptic robotic hand performing human-robot handshake with human-like agility," in *2017 IEEE/RSJ International Conference on Intelligent Robots and Systems (IROS)*, pp. 4626–4633, ISSN: 2153-0866.

[13] Z. Zhang, X. Chen, L. Shu, and X. Xu, "Adaptive readout approaches of resistive sensor array for wearable electronics applications," vol. 221, p. 113524. [Online]. Available: https://www.sciencedirect.com/science/article/pii/S0263224123010886

[14] Y. Yu, J. Li, S. A. Solomon, J. Min, J. Tu, W. Guo, C. Xu, Y. Song, and W. Gao, "All-printed soft human-machine interface for robotic physicochemical sensing," vol. 7, no. 67, p. eabn0495, publisher: American Association for the Advancement of Science. [Online]. Available: https://www.science.org/doi/10.1126/scirobotics.abn0495

[15] T. Luong, S. Seo, J. Jeon, C. Park, M. Doh, S. Park, F. Yumbla, and H. Moon, "Design and fabrication of an array of touch sensors for robotic applications," in *2023 IEEE 19th International Conference on Automation Science and Engineering (CASE)*, pp. 1–6, ISSN: 2161-8089. [Online]. Available: https://ieeexplore.ieee.org/abstract/document/10260487

[16] F. Vigni, E. Knoop, D. Prattichizzo, and M. Malvezzi, "The role of closed-loop hand control in handshaking interactions," vol. 4, no. 2, pp. 878–885. [Online]. Available: https://ieeexplore.ieee.org/document/8613850

[17] P. M. Khin, J. H. Low, M. H. Ang, and C. H. Yeow, "Development and grasp stability estimation of sensorized soft robotic hand," vol. 8, publisher: Frontiers. [Online]. Available: https://www.frontiersin.org/journals/robotics-and-ai/articles/10.3389/frobt.2021.619390/full

[18] K. Yamasaki, T. Shibata, and P. Hénaff, "Individual adaptation and social attributes in a handshake robot with CPG control," vol. 38, no. 17, pp. 1202–1217. [Online]. Available: https://doi.org/10.1080/01691864.2024.2384422

[19] M. Faisal, F. Laamarti, and A. El Saddik, "Digital twin haptic robotic arms: Towards handshakes in the metaverse," vol. 12, no. 12, p. 2603, publisher: Multidisciplinary Digital Publishing Institute. [Online]. Available: https://www.mdpi.com/2079-9292/12/12/2603

[20] M. Rennung and A. S. Göritz, "Prosocial consequences of interpersonal synchrony," publisher: Hogrefe Publishing. [Online]. Available: https://econtent.hogrefe.com/doi/10.1027/2151-2604/a000252

[21] L. K. Cirelli, K. M. Einarson, and L. J. Trainor, "Interpersonal synchrony increases prosocial behavior in infants," vol. 17, no. 6, pp. 1003–1011. [Online]. Available: https://onlinelibrary.wiley.com/doi/10.1111/desc.12193

[22] K. Fujiwara, M. Kimura, and I. Daibo, "Rhythmic features of movement synchrony for bonding individuals in dyadic interaction," vol. 44, no. 1, pp. 173–193. [Online]. Available: https://doi.org/10.1007/s10919-019-00315-0

[23] M. J. Hove and J. L. Risen, "It's all in the timing: Interpersonal synchrony increases affiliation," vol. 27, no. 6, pp. 949–960. [Online]. Available: http://guilfordjournals.com/doi/10.1521/soco.2009.27.6.949

[24] R. Mogan, R. Fischer, and J. A. Bulbulia, "To be in synchrony or not? a meta-analysis of synchrony's effects on behavior, perception, cognition and affect," vol. 72, pp. 13–20. [Online]. Available: https://www.sciencedirect.com/science/article/pii/S0022103116306114

[25] D. Fu, F. Abawi, P. Allgeuer, and S. Wermter, "Human impression of humanoid robots mirroring social cues," in *Companion of the 2024 ACM/IEEE International Conference on Human-Robot Interaction*. ACM, pp. 458–462.

[26] M. Jouaiti, C. L. Nehaniv, and K. Dautenhahn, "What do we mean by synchrony in human–robot interaction research?: Towards a unifying framework," vol. 25, no. 3, pp. 313–339, publisher: John Benjamins Publishing Company. [Online]. Available: https://benjamins.com/catalog/is.24011.jou

[27] S. Watatani, H. Nagano, Y. Tazaki, and Y. Yokokohji, "Tele haptic handshake using distributed pressure presentation device and mutual interaction pressure model," vol. 14, no. 3, p. 537, publisher: Multidisciplinary Digital Publishing Institute. [Online]. Available: https://www.mdpi.com/2079-9292/14/3/537

[28] F. J. Ruiz-Ruiz, J. Ventura, C. Urdiales, and J. M. Gómez-de Gabriel, "Compliant gripper with force estimation for physical human–robot interaction," vol. 178, p. 105062. [Online]. Available: https://www.sciencedirect.com/science/article/pii/S0094114X22003093

[29] A. Pequeno-Zurro, E. Chicca, and O. Palinko, "Tactile sensing improves handshake between humans and robots," in *Social Robotics*. Springer Nature, pp. 145–158.

[30] J. Avelino, T. Paulino, C. Cardoso, R. Nunes, P. Moreno, and A. Bernardino, "Towards natural handshakes for social robots: human-aware hand grasps using tactile sensors," vol. 9, no. 1, pp. 221–234, publisher: De Gruyter Open Access Section: Paladyn. [Online]. Available: https://www.degruyterbrill.com/document/doi/10.1515/pjbr-2018-0017/html

[31] B. Rammstedt and O. P. John, "Measuring personality in one minute or less: A 10-item short version of the big five inventory in english and german," *Journal of Research in Personality*, vol. 41, no. 1, p. 203–212, Feb. 2007.

[32] P. M. Desmet, M. H. Vastenburg, and N. Romero, "Mood measurement with pick-a-mood: review of current methods and design of a pictorial self-report scale," vol. 14, no. 3, p. 241. [Online]. Available: http://www.inderscience.com/link.php?id=79751

[33] Y. She, S. Song, H.-J. Su, and J. Wang, "A comparative study on the effect of mechanical compliance for a safe physical human–robot interaction," *Journal of Mechanical Design*, vol. 142, no. 6.